World Journal of Engineering Research and Technology
WJERT
www.wjert.org
SJIF Impact Factor: 5.924

FINITE ELEMENT ANALYSIS OF EXTREME STATE OF BALL VALVE

Ren-He Tao[1], Jian-Yang Song[2], Kai-Yuan Zhang[2], Hao-Nan Xu[2], Can-Fei Wang[1]*

[1]Zhejiang Institute of Mechanical & Electrical Engineering Co., Ltd, Hangzhou 310002, China.

[2]College of Mechanical Engineering, Quzhou University, Quzhou, 324000, China.

Article Received on 20/02/2020 **Article Revised on 10/03/2020** **Article Accepted on 30/03/2020**

***Corresponding Author**
Can-Fei Wang
Zhejiang Institute of Mechanical & Electrical Engineering Co., Ltd, Hangzhou 310002, China.

ABSTRACT

In this study, Solidworks software was used to calculate and analyze the stress and strain of the valve port of the ball valve, and the numerical characteristics of the stress, strain and displacement of the ball valve were preliminarily estimated. The results of this study will provide a good basis for further research on numerical characteristics of ball valve at different positions. By studying the preliminary findings of ball valve in the fully open and fully closed in both cases, the stress, strain and displacement of the valve port suffered under the grid as a variable stress change with the increase of grid number , strain and displacement data in the grid number increase after the change is small, the material is a greater difference between the values of maximum stress under variable, while the smallest stress value were similar, strain and displacement of maximum minimum value difference is not large, in the variable for the load stress and strain when the maximum and the minimum and maximum displacement and load force has a positive correlation. The minimum displacement value does not increase with the increase of the loading force, and remains unchanged.

KEYWORDS: ball valve, extreme condition, finite element analysis.

INTRODUCTION

Ball valve.[1,2] belongs to a throttle valve, because the ball has a cylindrical shape and called it, it is simple structure, small volume, light weight, compact and reliable. It has two sealing

surface, and the ball valve sealing surface materials are widely used in a variety of plastics. And it has good sealing, can achieve complete sealing, has been widely used in vacuum system. In addition, it is easy to operate and quick to open and close. It only needs to rotate 90° from full open to full close to facilitate remote control. When fully open or fully closed, the sealing surface of the valve body and valve seat is isolated from the medium. When the medium passes through, it will not cause the erosion of the sealing surface of the valve. In addition, its main feature is effective throttling, minimize drawing to minimize erosion of valve and seat. It is mainly used in closed and frequent switch and throttling action when fluid flow must be controlled. In the study of ball valve, the paper research key points from ball valve flow caused by the body pressure pulsation test,[3,4] mainly study of flow on the body of the key pressure points,[5,6] also have to work under high pressure ball valve, improve research about the structure of the body, and the ball valve seal damage cause analysis research.[7,8] In this paper, the strain and stress of the ball valve at the valve orifice are different under the condition of fully open and completely closed. Based on this, the Solidworks[9] model is used to conduct numerical calculation and analysis on the ball valve under the extreme conditions of full open and full closed, and obtain the relevant data. In this paper, the influence of material, load and grid on the stress, strain and displacement of the ball valve at the same position is studied in the two extreme states of fully closed and fully open.

Physical model

The ball valve model

In this paper, the main research object is the common ball valve, and three-dimensional modeling software is used to model the ball valve, the specific size is shown in figure 1.

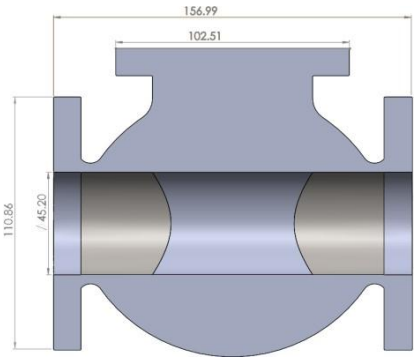

Fig. 1: basic dimensions of ball valve.

The three-dimensional section of the ball valve with fully open and fully closed is shown in

figure 2.

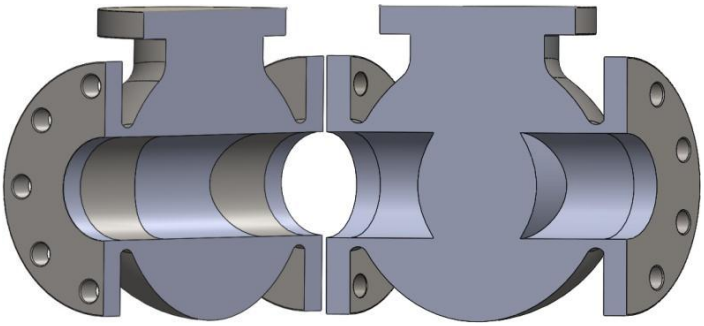

(a)Opening (b)Closing

Fig. 2: Ball valve 3d modeling diagram.

1.2 Calculation method

In this article, the main use of Solidworks simulation[10] finite element analysis of plug-in is analyzed, the model of finite element analysis of parts generated by actual examples, and are added to the model of concrete materials and loads as well as the meshing, generated by an example, the control mesh material and load under the change of single variable method to study the three variables of ball valve mouth of stress and strain and displacement value.

In this paper, finite element analysis is carried out on the ball valve model in two extreme states of fully open and completely closed, and the actual simulation is carried out. The three-dimensional model of ball valve is added with the actual material, and the load is determined at the valve port in the specific position, and the grid division is changed controllable. In this paper, the effects of mesh division, load size and material properties on the stress, strain and displacement of the ball valve under the same load were studied. The results of this study will also provide a good basis for further research on the numerical characteristics of ball valves at different load positions.

Full opening Materials effect

Before the numerical analysis, three materials of cast stainless steel and the PE high-density plastic and titanium alloy were selected, respectively, as shown in table 1, table 2 and table 3.

Table 1: Cast stainless steel properties.

Property	Numerical value	Unit
Elastic modulus	1.9×10^{-11}	N/m^2
Poisson ratio	0.26	Not applicable
Medium shear modulus	7.9×10^{10}	N/m^2
Mass density	7700	Kg/m^3
Coefficient of thermal expansion	9.5×10^{-6}	/k
Thermal conductivity	37	W/(m·k)
Specific heat capacity	520	J/(kg·k)

Table 2: PE high density plastic properties.

Property	Numerical value	Unit
Elastic modulus	1.103×10^{11}	N/m^2
Poisson ratio	0.31	Not applicable
Medium shear modulus	4.8×10^{10}	N/m^2
Mass density	4480	Kg/m^3
Coefficient of thermal expansion	9.4×10^{-6}	/k
Thermal conductivity	7.8	W/(m·k)
Specific heat capacity	530	J/(kg·k)
Strong strength	8.61×10^{8}	N/m^2
Compressive strength	8.3×10^{8}	N/m^2
Yield strength	8.27×10^{8}	N/m^2

Table 3: Ti-5Al-2.5Sn properties.

Property	Numerical value	Unit
Elastic modulus	1.07×10^{9}	N/m^2
Poisson ratio	0.4101	Not applicable
Medium shear modulus	3.772×10^{8}	N/m^2
Mass density	952	Kg/m^3
Thermal conductivity	0.461	W/(m·k)
Specific heat capacity	1796	J/(kg·k)
Strong strength	2.21×10^{7}	N/m^2

It can be seen from the properties of the three materials in the table that the properties of the three materials differ greatly in various aspects, so the numerical analysis of the same stress value and the same cell at the same position is more valuable. In order to obtain the stress situation of ball valve, Solidworks simulation[11] is adopted in this paper to simulate the change of stress, strain and displacement of the valve port when the ball valve is fully opened. In this paper, the Solidworks simulation plug-in is used to establish a static stress calculation example to simulate and analyze the relationship between each value and grid size. Solidworks material library is used to add three different materials of cast stainless steel and PE high-density plastics and Ti-5Al-2.5Sn to the valve port model of ball valve profile respectively, and apply 100N load on three materials uniformly. Then, the change of stress,

strain and displacement under different materials is obtained by dividing the same cell.

Solidworks simulation was used to simulate and analyze the changes of stress, strain and displacement of valve orifice under different materials when the ball valve is fully opened and the grid is divided into 50,000 cells, as shown in figure 3, figure 4 and figure 5 below.

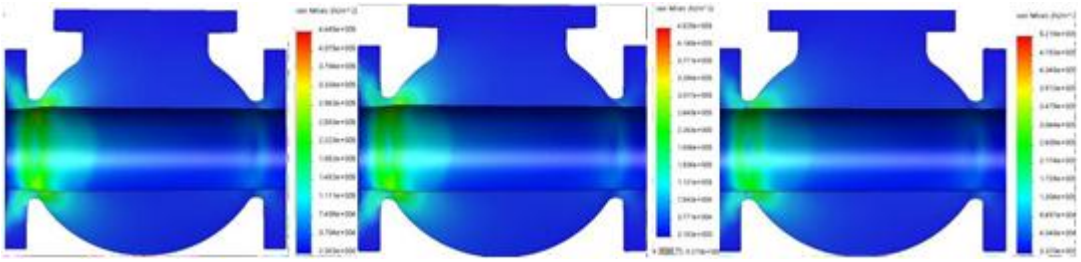

(a)Cast stainless steel (b)Ti-5Al-2.5Sn (c)PE high density plastics

Fig. 3: Stress distribution of three material at 50, 000 cells.

According to the stress distribution cloud diagram of three materials in figure 1 divided into 50,000 grids after loading, the data in the figure shows that. In the cast stainless steel material, the maximum stress is 4.445×10^5N/m^2, the minimum stress is 2.383N/m^2, and in the Ti-5Al-2.5Sn material, the maximum stress is 4.525×10^5N/m^2, and the minimum stress is 3.183N/m^2.In high-density PE plastic material under the maximum stress value of 5.218×10^5N/m^2, minimum 3.320N/m^2, so compare the three kinds of materials available, the stress distribution under the value under the three different material of maximum stress difference is bigger, the maximum stress value of measurement under the cast stainless steel material with al Ti-5Al-2.5Sn material under the maximum stress value is 8,000 N/m^2, and differ with high-density PE plastic material under the maximum stress value of 77,300 N/m^2, and the minimum stress value of the three.

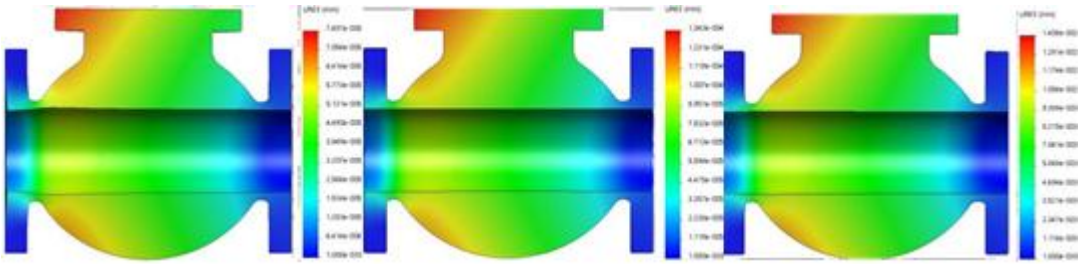

(a)Cast stainless steel (b)Ti-5Al-2.5Sn (c)PE high density plastic

Fig. 4: Displacement distribution of three material at 50, 000 cells.

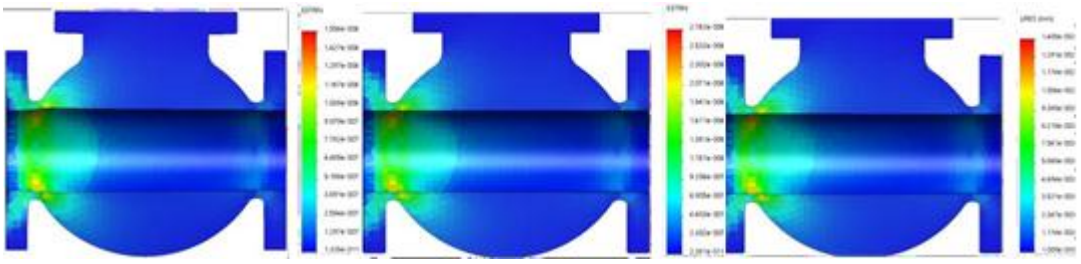

(a)Cast stainless steel (b)Ti-5Al-2.5Sn (c)PE high density plastic

Fig. 5: Strain distribution of three material at 50, 000 cells.

It can be known from the strain and displacement distribution cloud maps of three materials in figure 4 and figure 5 when the grid is divided into 50,000 grids after loading. The maximum displacement value and minimum value of the three different kinds of materials were tiny, and the maximum displacement of the PE high plastic material was different from that of the maximum displacement value of the steel and casting stainless steel, and the maximum and minimum strain value of the PE high plastic material was also small compared to the other two, and the displacement and strain value of different materials in the same grid was not very different.

Grids effect

100N load was added to the valve port, and Ti-5Al-2.5Sn material was applied. The stress cloud diagram distribution under different grids was shown in figure 6.

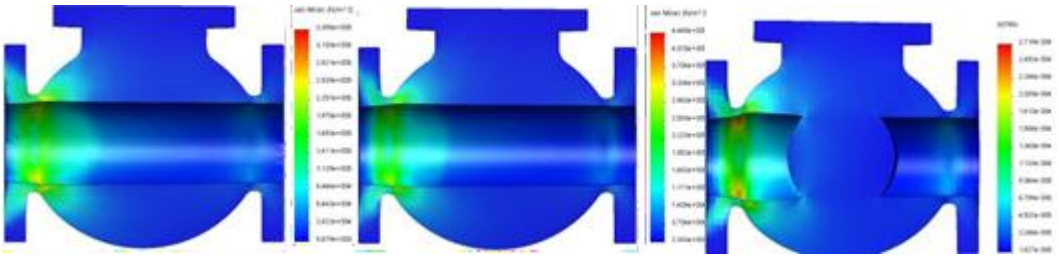

(a)10，000 cell (b)50，000 cell (c)100，000 cell

Fig. 6: Stress distribution of Ti-5Al-2.5Sn under three grids.

It can be seen from the figure that after loading Ti-5Al-2.5Sn, the maximum stress in 10000 cells, 50000 cells and 100000 cells is 3.385×10^5 N/m^2,4.445×10^5 N/m^2, 2.719×10^4 N/m^2,

respectively, and the minimum stress is 9.679×10^{0} N/m^2,2.383×10^{0} N/m^2,1.827×10^{9}N/m^2. Therefore, the comparison of these three groups of data shows that in the stress analysis of valve port under Ti-5Al-2.5Sn material, the selection and division of cell has a great influence on the displacement change.

100N load was added to the valve port and Ti-5Al-2.5Sn material was applied. The distribution of displacement cloud map under different grids was shown in figure 7.

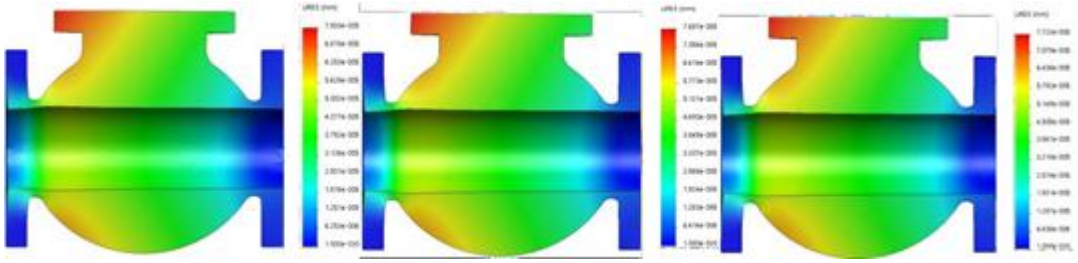

(a)10000 cell (b)50000 cell (c)100000 cell

Fig. 7: Displacement distribution of Ti-5Al-2.5Sn under three grids.

The maximum value of displacement distribution of Ti-5Al-2.5Sn is 1.309×10^{-4}mm in 10000 cells, the minimum value is 1.000×10^{-30}mm, the maximum value is 1.347×10^{-4}mm in 50,000 cells, the minimum value is 1.000×10^{-30}mm, and the maximum value is 1.347×10^{-4}mm in 100,000 cells, the minimum value is1.000×10^{-30}mm.In the above three groups of data, the displacement change value did not change significantly with the increase of the number of cells, so the comparison of the three groups of data showed that the selection and division of cells had little influence on the displacement change in the analysis of valve port displacement under Ti-5Al-2.5Sn material.

100N load was added to the valve port and Ti-5Al-2.5Sn material was applied. The strain cloud diagram distribution under different grids was shown in figure 8.

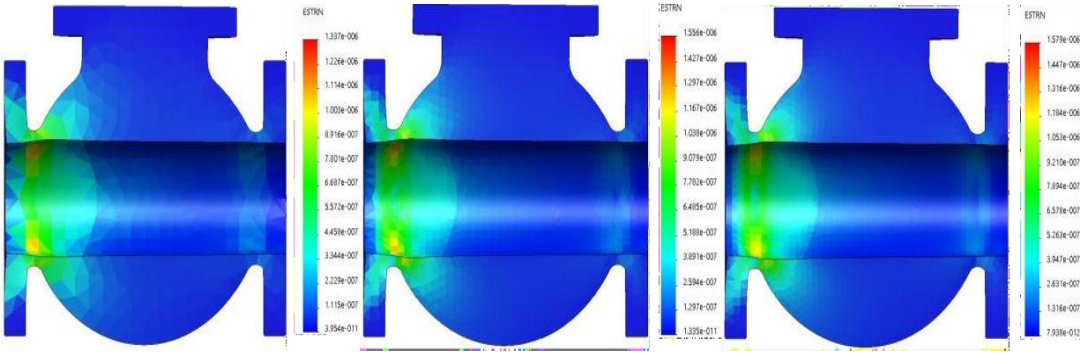

(a)10，000 cell (b)50，000 cell (c)100，000 cell

Fig. 8: Strain distribution of Ti-5Al-2.5Sn under three grids.

It can be seen from the figure that the maximum and minimum values of strain under 10000 cells, 50000 cells and 100000 cells are 2.384×10^{-6},7.358×10^{-11}, 2.762×10^{-6},2.381×10^{-11}, 2.813×10^{-6}, 1.416×10^{-11}, respectively. Therefore, by comparing the three groups of data, it can be concluded that the change of strain has little relationship with the selection of cell division, and the size of the selected cell has little influence on it.

2.3 Loads effect

After the valve port section is divided into 100,000 cells, cast stainless steel shall be applied, as shown in figure 9.

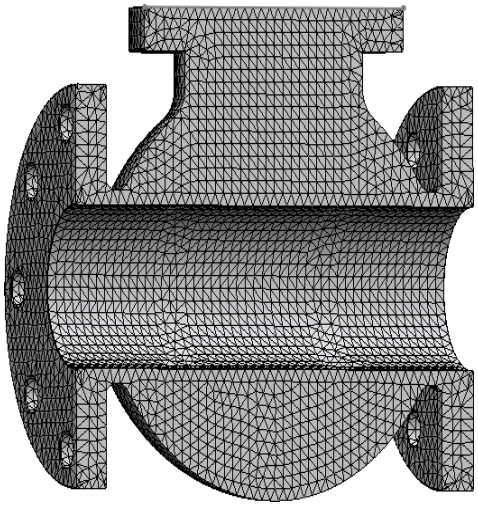

Fig. 9: 3D model after grid division.

The stress nephogram distribution under different loads is shown in figure 10.

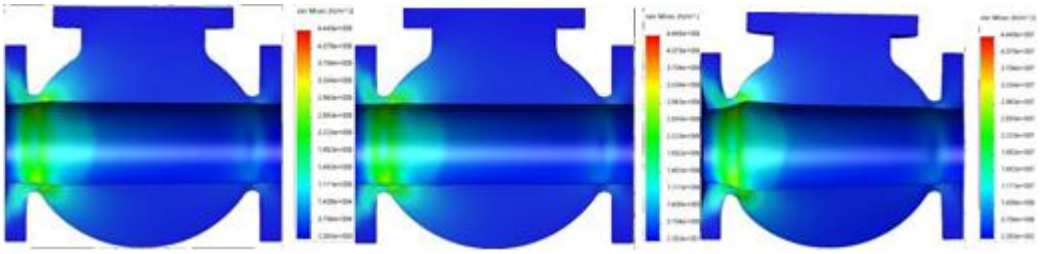

(a) Load of 100N (b)Load of 1000N (c)Load of 10000N

Fig. 10: Stress distribution of cast stainless steel under three loads.

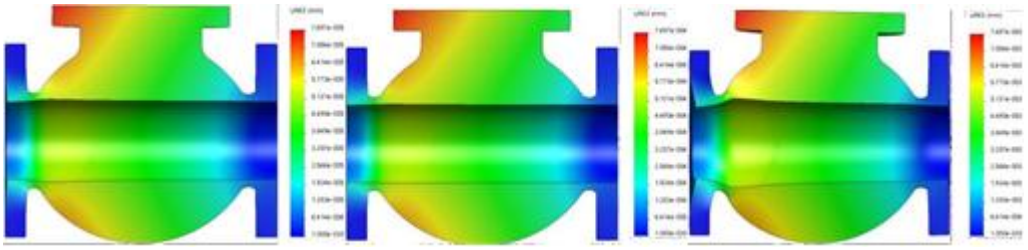

(a) Load of 100N (b)Load of 1000N (c)Load of 10000N

Fig. 11: Displacement distribution of cast stainless steel under three loads.

The distribution of displacement nephogram under different loads is shown in figure 11.

The distribution of strain nephogram under different loads is shown in figure 12.

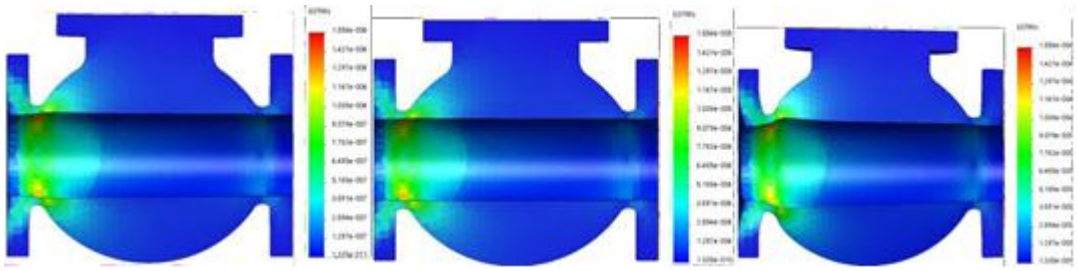

(a)Load of 100N (b)Load of 1000N (c)Load of 10000N

Fig. 12: Strain distribution of cast stainless steel under three loads.

As can be seen from the data in figure 10, figure 11 and figure 12, the maximum stress of the data in the figure is $4.445\times10^{5}N/m^{2}$, $4.445\times10^{6}N/m^{2}$, $4.445\times10^{7}N/m^{2}$, and the minimum stress is $2.383\times10^{0}N/m^{2}$, $2.383\times10^{1}N/m^{2}$, $2.383\times10^{2}N/m^{2}$. It can be seen that the maximum and minimum stresses increase by 10 times as the load increases, so the maximum and minimum stresses have a linear relationship with the load force. In addition, in the distribution of the cloud map of the strain, we can also see the relation of numerical multiplication. When the load number is increased from 10 times, the maximum and

minimum strain also increase by 10 times. For the displacement, the maximum value has this relation.

3 Complete closing

3.1 Materials effect

Before the numerical analysis, three materials of cast stainless steel PE high-density plastic titanium alloy were selected, respectively, as shown in table 4, table 5 and table 6.

Table 4: Cast stainless steel properties.

Property	Numerical value	Unit
Elastic modulus	1.9×10^{-11}	N/m^2
Poisson ratio	0.26	Not applicable
Medium shear modulus	7.9×10^{10}	N/m^2
Mass density	7700	Kg/m^3
Coefficient of thermal expansion	9.5×10^{-6}	/k
Thermal conductivity	37	W/(m·k)

Table 5: Ti-5Al-2.5Sn properties.

Property	Numerical value	Unit
Elastic modulus	1.07×10^{9}	N/m^2
Poisson ratio	0.4101	Not applicable
Medium shear modulus	3.772×10^{8}	N/m^2
Mass density	952	Kg/m^3
Thermal conductivity	0.461	W/(m·k)
Specific heat capacity	1796	J/(kg·k)
Strong strength	2.21×10^{7}	N/m^2

Table 6: PE High density plastic.

Property	Numerical value	Unit
Elastic modulus	1.103×10^{11}	N/m^2
Poisson ratio	0.31	Not applicable
Medium shear modulus	4.8×10^{10}	N/m^2
Mass density	4480	Kg/m^3
Coefficient of thermal expansion	9.4×10^{-6}	/k
Thermal conductivity	7.8	W/(m·k)
Specific heat capacity	530	J/(kg·k)
Strong strength	8.61×10^{8}	N/m^2
Compressive strength	8.3×10^{8}	N/m^2
Yield strength	8.27×10^{8}	N/m^2

It can be seen from the properties of the three materials in the figure that the properties of the three materials differ greatly in various aspects, so the numerical analysis of the same stress value and the same cell at the same position is more valuable. In order to obtain the strain

stress and displacement of the ball valve when it is completely closed, Solidworks simulation is adopted in this paper to simulate the stress strain and displacement of the valve port when the ball valve is completely closed. In this paper, the static stress calculation example is established through Solidworks simulation plug-in, and the relationship between each value and grid size is simulated and analyzed. Solidworks material library is used to add three different materials of cast stainless steel PE high-density plastics and Ti-5Al-2.5Sn to the valve port model of ball valve profile respectively, and apply 100N load on three materials uniformly. Then, the change of stress, strain and displacement under different materials is obtained by dividing the same cell.

Solidworks simulation was used to simulate and analyze the changes of stress, strain and displacement of valve orifice under different materials when the ball valve is fully opened and the grid is divided into 100,000 cells, as shown in figure 13, figure 14and figure 15 below.

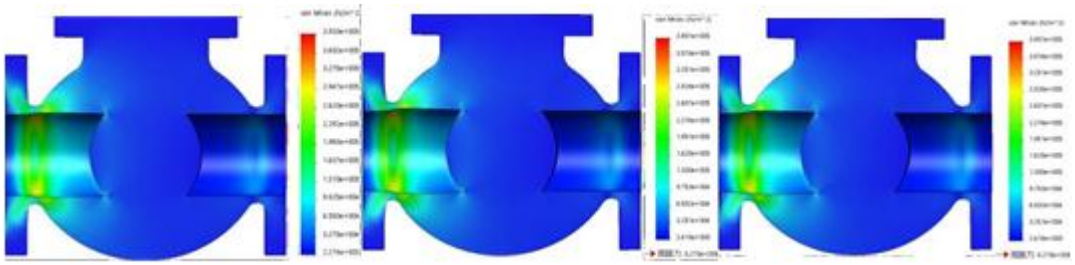

(a)Cast stainless steel (b)Ti-5Al-2.5Sn (c)PE high density plastics

Fig. 13: Stress distribution of three material at 100, 000 cells.

By three kinds of materials in figure11 after loading the distribution in the grid is divided into 50000 grid, the stress distribution under the cloud data in figure show that under the cast stainless steel material, the maximum stress value$3.930\times10^{5}N/m^{2}$, the minimum stress is $2.274N/m^{2}$, Ti-5Al-2.5Sn material, the maximum stress value of $3.901\times10^{5}N/m^{2}$, the minimum stress value of $2.418N/m^{2}$, in high-density PE plastic material under the maximum stress value of $3.870\times10^{5}N/m^{2}$, minimum $2.423N/m^{2}$.So contrast under three kinds of materials available value of the stress distribution, the maximum stress under three different material value difference is bigger, the maximum stress value of measurement under the cast stainless steel material with al Ti-5Al-2.5Sn material under the maximum stress value from $2.9\times10^{3}N/m^{2}$, and Ti-5Al-2.5Sn material and high-density PE plastic material under the maximum stress value difference between $3.1\times10^{3}N/m^{2}$, and the minimum stress value of the three.

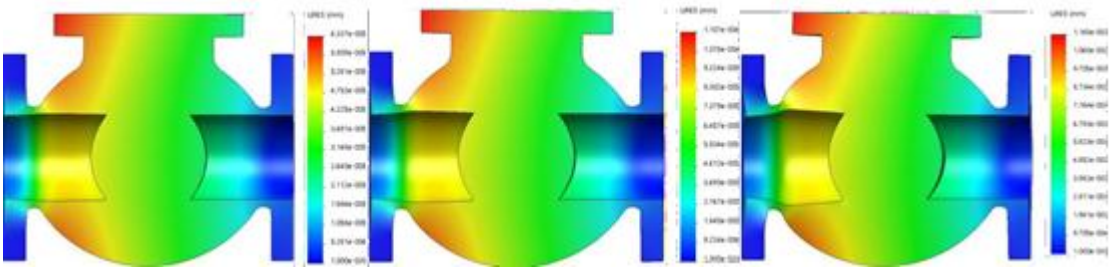

(a)Cast stainless steel (b)Ti-5Al-2.5Sn (c)PE high density plastic

Fig. 14: Displacement distribution of three material at 100, 000 cells.

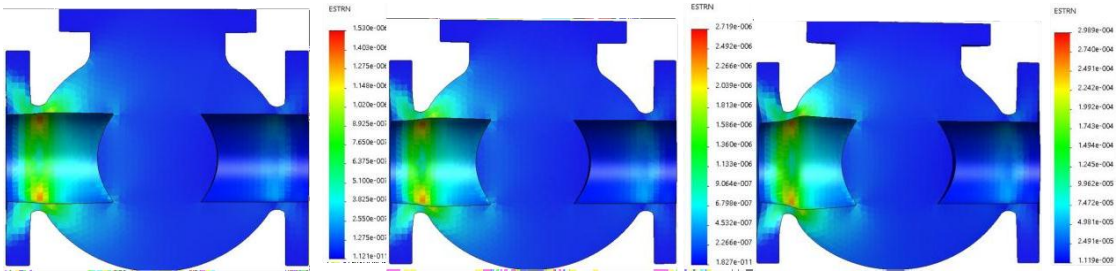

(a)Cast stainless steel (b)Ti-5Al-2.5Sn (c)PE high density plastics

Fig. 15: Strain distribution of three material at 100, 000 cells.

It can be known from the strain and displacement distribution cloud maps of three materials in figure 12 and figure 13 when the grid is divided into 50000 grids after loading. The maximum and minimum values of the displacement and strain values of the three materials under the same load. Therefore, by comparing the stress distribution values of the three materials, it can be concluded that the maximum displacement and minimum values of the three materials differ slightly. Which the maximum displacement value of high-density PE plastic material and al Ti-5Al-2.5Sn material and cast stainless steel material maximum displacement difference between1.00-1.43mm, and high-density PE plastic material under the maximum and minimum strain value compared with the other two differentiae also is very small, analysis on displacement and strain values, the same values of the displacement and strain of different material under grid data are very small.

3.2 Grids effect

100N load is added to the valve port and cast stainless steel is applied. The stress nebugram distribution under different grids is shown in figure 16.

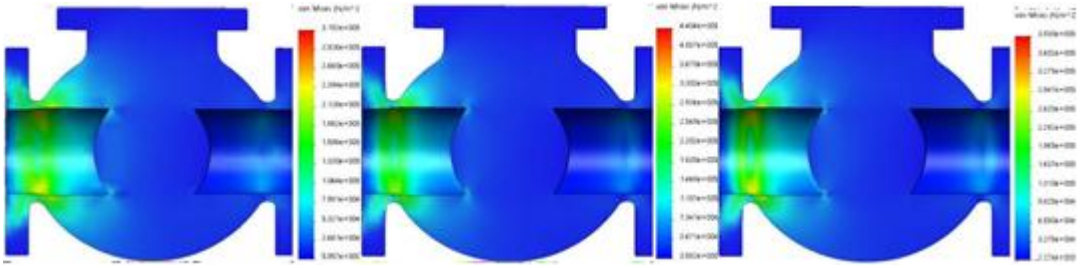

(a)10000 cell (b)50000 cell (c)100000 cell

Fig. 16: Stress distribution of cast stainless steel under three grids.

It can be seen from the figure that after loading cast stainless steel, the maximum stress in 10000 cells, 50000 cells and 100000 cells is 3.192×10^{5} N/m^2,4.404×10^{5} N/m^2, 3.930×10^{4} N/m^2, respectively, and the minimum stress is 5.957N/m^2,3.582N/m^2,2.274N/m^2.So the data can be cast stainless steel under different grid stress distribution of the maximum value is large, and the minimum under three kinds of grid numerical difference is very small, so the casting stainless steel material compared to the three sets of data on the valve mouth stress analysis of the choice of cell division to a maximum stress change, less influence to the minimum.

100N load is added to the valve port and cast stainless steel material is applied. The distribution of displacement cloud diagram under different grids is shown in figure 17.

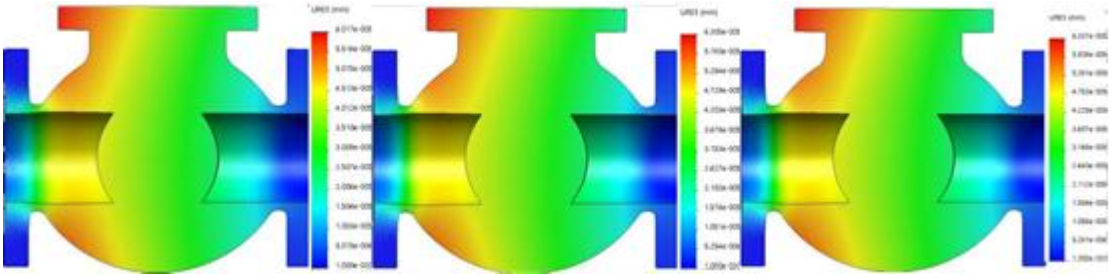

(a) 10000 cell (b)50000 cell (c)100000 cell

Fig. 17: Displacement distribution of cast stainless steel under three grids.

As can be seen from the figure, the maximum displacement of cast stainless steel in 10000 cells, 50000 cells and 100000 cells is 6.017×10^{-5}mm,6.305×10^{-5}mm, 6.337×10^{-5}mm, respectively, and the maximum displacement is 1.000×10^{-30}mm,2.383×10^{-30} mm,1.000×10^{-30}mm. In the above three groups of data, the displacement change value did not change much with the increase of cell number, so the comparison of the three groups of data shows that the selection of cell has little influence on the displacement change in the analysis of valve port displacement of cast stainless steel.

100N load was added to the valve port and cast stainless steel was applied. The strain cloud diagram distribution under different grids was shown in figure 18.

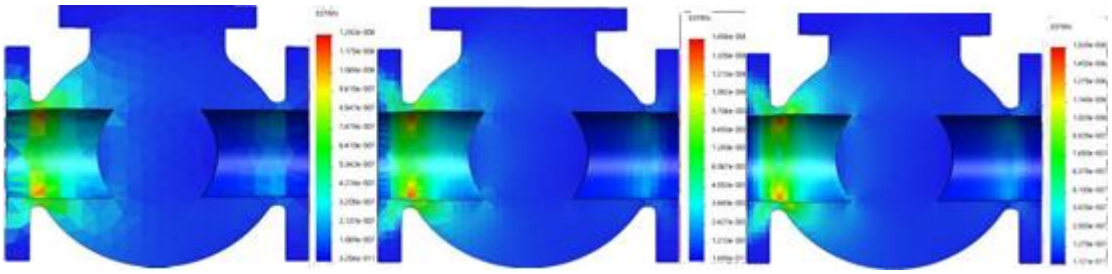

(a) 10000 cell (b) 50000 cell (c)100000 cell

Fig. 18: Strain distribution of cast stainless steel under three grids.

It can be seen from the figure that the maximum and minimum stress values in 10000 cells, 50000 cells and 100000 cells are 1.282×10^{-6}, 3.256×10^{-11}, 1.456×10^{-6},1.685×10^{-11}, 1.530×10^{6}, 1.121×10^{-11}, respectively. Therefore, by comparing the three groups of data, it can be concluded that the change of strain has little relationship with the selection of cell division, and the size of the selected cell has little influence on it.

3.3 Loads effect

After the valve port section is divided into 100,000 cells, cast stainless steel shall be applied, as shown in figure 19.

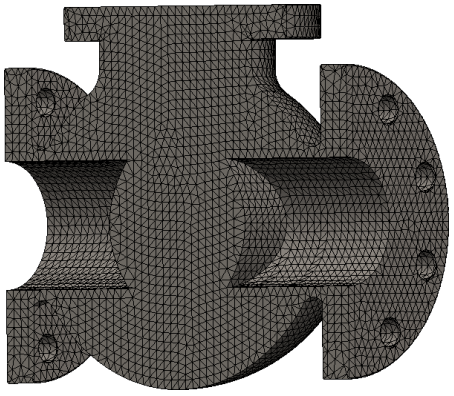

Fig. 19: 3d model after grid division.

The stress distribution under different loads is shown in figure 20.

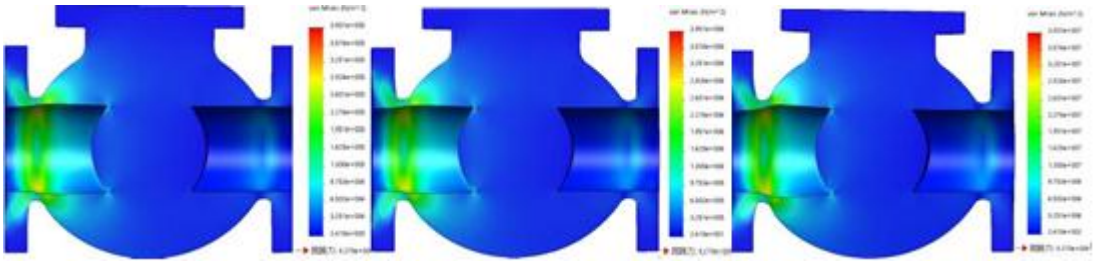

(a) Load of 100N (b) Load of 1000N (c) Load of 10000N

Fig. 20: Stress distribution of cast stainless steel under three loads.

The distribution of displacement under different loads is shown in figure 21.

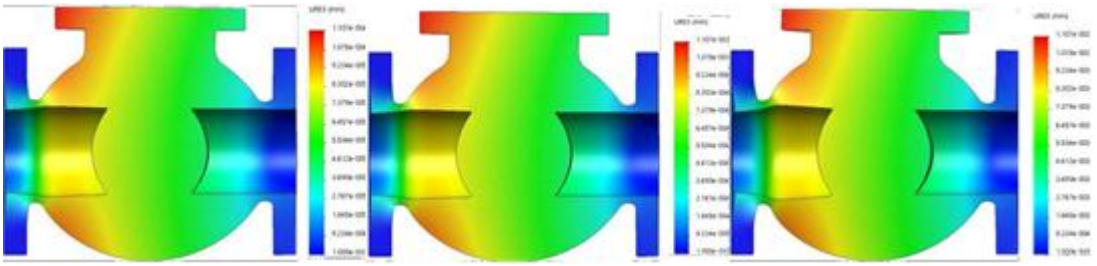

(a) Load of 100N (b)Load of 1000N (c)Load of 10000N

Fig. 21: Displacement distribution of cast stainless steel under three loads.

The distribution of strain under different loads is shown in figure 22.

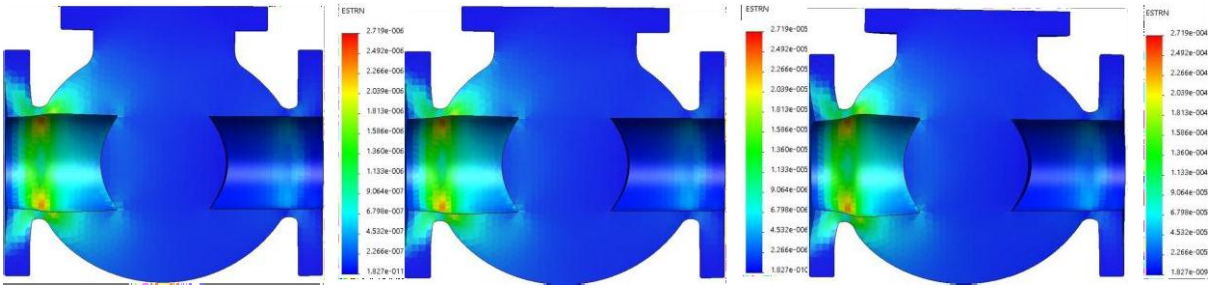

(a)Load of 100N (b)Load of 1000N (c)Load of 10000N

Fig. 22: Strain distribution of cast stainless steel under three loads.

Figure 18, figure 19 and figure 20 show that the maximum strain of cast stainless steel under loading conditions of 100N, 1000N and 10000N is 2.719×10^{-6}, 2.719×10^{5}, 2.719×10^{5}, and the minimum value is 1.827×10^{-11}, 1.827×10^{-10}, 1.827×10^{-9}, respectively .It can be seen that the maximum and minimum stresses increase by 10 times as the load increases, so the maximum and minimum stresses have a linear relationship with the load force. In addition, in the

distribution of the cloud map of the strain, we can also see the relation of numerical multiplicative number. When the load number is increased from 10 times, the maximum and minimum values of the strain also increase by 10 times. For displacement, the maximum value has this relation, and the minimum value does not increase with the increase of the loading force.

4 CONCLUSION

In this paper, Solidworks software is used to perform numerical calculation and analysis on the ball valve when it is fully open and completely closed to obtain relevant data. Thus the strain stress and displacement data are analyzed in the same material with the same load and different grids, and the same load, same grid number, different materials and the same material, same mesh number, different load of three conditions. Through numerical analysis, it is preliminarily found that under the same material, same load and different grids, the stress increases with the increase of grid number, and the strain and displacement data change slightly after the increase of grid number. In the case of the same load and the same number of grids and different materials, by comparing the values of stress, strain and displacement of the three materials with large difference in the three properties, it is found that the maximum stress values of the three materials have great difference, while the minimum stress values have little difference, and the maximum and minimum values of strain and displacement have little difference. In the case of the same material, the same number of grids and different loads, the data analysis shows that the maximum and minimum stress and strain increase by 10 times as the load increases by 10 times. Therefore, the maximum and minimum values of stress and strain are positively correlated with the loading force. However, only the maximum displacement has this relation, and the minimum displacement does not increase with the increase of the loading force.

REFERENCES

1. Jingni Lu, Shan Tu, Hongjuan Wang, et al. Flow characteristics and structural optimization of ball regulating valve[J]. Chinese journal of power engineering, 2017; (12): 963-968, 982.
2. Anonymous. Ball valve offers upped p`erformance[J]. Engineering and Mining Journal, 2017; 220(6): 220-223.
3. Daniel Moses, Ghulam Haider, John Henshaw. An investigation of the failure of a 1/4" ball valve[J]. Engineering Failure Analysis, 2019; 100(5): 393-405.

4. Shan Tu. Experimental study on pressure pulsation of valve body key points caused by ball regulating valve flow[J]. Thermal science and technology, 2019; 3(4): 12-15.
5. S. Bagherifard, I. Fernández Pariente, M. Guagliano. Failure analysis of a large ball valve for pipe-lines[J]. Engineering Failure Analysis, 2013; 11(32): 167-177.
6. Coker P J. Ball-valve tertiary seal assembly and method[J]. Sealing technology, 2017; 24(9): 15-17.
7. Elsevier journal. Next generation of compact ball valve[J]. World Pumps, 2017; 54(4): 10-12.
8. Baoling Cui, Zhe Lin, Zuchao Zhu, et al. Influence of opening and closing process of ball valve on external performance and internal flow characteristics[J]. Experimental thermal and fluid science, 2017; 114(80): 193-202.
9. Jinquan Zhu. Application and research of Solidworks software in mechanical design[J]. New technology and new process, 2009; 44(2): 41-44.
10. Yongzhi Li. 3D modeling design of slurry pump volute [J]. Mechanical design and manufacturing, 2008; 72(4): 46-47.
11. Fengwen Cheng. Parametric design of mechanical parts based on Solidworks[J]. Modern manufacturing engineering, 2016; 36(2): 18-19.